

A new assessment of European forests carbon exchanges by eddy fluxes and artificial neural network spatialization

DARIO PAPALE and RICCARDO VALENTINI

Laboratory of Forest Ecology, Department of Forest Environment Science and Resource, University of Tuscia, DISAFRI, Via Camillo de Lellis, 01100 Viterbo, Italy

Abstract

Recently flux tower data have become available for a variety of ecosystems under different climatic and edaphic conditions. Although Flux tower data represent point measurements with a footprint of typically $1\text{ km} \times 1\text{ km}$ they can be used to validate models and to spatialize biospheric fluxes at regional and continental scales. In this paper we present a study where biospheric flux data collected in the EUROFLUX project were used to train a neural network simulator to provide spatial ($1\text{ km} \times 1\text{ km}$) and temporal (weekly) estimates of carbon fluxes of European forests at continental scale. The novelty of the approach is that flux data were used to constrain and parameterize the neural network structure using a limited number of input driving variables. The overall European carbon uptake from this analysis was 0.47 Gt C yr^{-1} with distinctive differences between boreal and temperate regions. The length of the growing season is longer in the south of Europe (about 32 weeks), compared with north and central Europe, which have a similar length-growing season (about 27 weeks). A peak in respiration was depicted in spring at continental scale as a coherent signal which parallel the construction respiration increase at the onset of the season as usually shown by leaf level measurements.

Keywords: biogeochemical cycles, biospheric exchanges, carbon fluxes, eddy covariance, micro-meteorology, neural network

Received 4 September 2002; revised version received and accepted 3 October 2002

Introduction

Several international efforts are today underway to construct a 'carbon data assimilation system' where models and observations are included in an optimization scheme to provide robust estimates of carbon fluxes at high resolution in both space and time scales.

Within the carbon cycle research community two quite distinct modelling techniques in a 'diagnostic' mode are used to estimate net land-atmosphere CO_2 fluxes. In 'inverse studies', atmospheric CO_2 measurements are used in conjunction with atmospheric transport modelling. These studies produce useful estimates of the large-scale geographical distribution of sources and sinks of carbon (Bousquet *et al.*, 2000), but they are unconstrained by physiological and ecological processes, and cannot currently provide good estimates at the policy-relevant

scale of countries. In 'forward modelling', models of land carbon uptake and release are developed based on an understanding of the relevant processes (e.g. the response of photosynthesis to CO_2 , the response of microbial respiration to climate), and then these models are integrated forward in time to produce predictions of the temporal and spatial variability of land-carbon sinks (Cramer *et al.*, 2001). Estimates of the land carbon balance produced by forward modelling to the current day are constrained by the understanding of the system embodied in the model (e.g. conservation of carbon and nitrogen), but not constrained by any direct observations of the carbon cycle (e.g. flux measurements, forest inventories, CO_2 flask measurements).

Artificial neural networks are a fast expanding field that have applications in many fields, from natural science disciplines (physics, biology, chemistry, etc.) to socio-economic science (literature, language, social studies, etc.) (Bishop, 1995; Demuth & Beale, 2000). Neural networks have great potential in biology and ecology

Correspondence: D. Papale, fax +39 0761 357389, e-mail: darpap@unitus.it

because they are able to represent the complexity of phenomena in examination (Lek & Guégan, 2000). Normally in such complex systems the manifestation of a function, or a property of the organism, represents the arranged effect of multiple nonlinear factors, which become activated to a given degree only in response to particular external circumstances.

Traditional systems of simulation, based on mechanistic models or statistical relationship, have great difficulty reproducing the complex responses of organisms. In this paper we present a preliminary study where biospheric flux data collected in the EUROFLUX project were used to train a neural network simulator to provide spatial (1 km × 1 km) and temporal (weekly) estimates of carbon fluxes of European forests. The novelty of the approach is that flux data were used to constrain and parameterize the neural network structure using a limited number of input driving variables. Since flux data were collected at high frequency (every half an hour) in 16 different forest ecosystems the time domain was a good replacement for the spatial variability. This means that when combined, the variability in response to climate at each flux site can be used to reproduce the effects of climate diversity within the European continent.

The work so far is at a preliminary stage thus results have to be viewed in the light of development of a new methodology rather than an established method to provide a final answer to the European continental carbon balance. However, here we present results consistent with other independent estimates of the carbon balance of continental Europe.

Methodology

What is an artificial neural network (ANN)?

Much of the inspiration for ANNs came from the desire to produce artificial systems capable of sophisticated, computations similar to those that the human brain performs, thereby possibly enhancing our understanding of the human brain.

There is no universally accepted definition of an ANN. However, it is generally accepted that an ANN is a network of many simple processing elements ('units' or 'nodes'), each having a small amount of local memory. The units, often organized in layers, are connected by communication channels ('connections') and operate only on their local data and on the inputs they receive via the connections (Fig. 1). Most ANNs have training rules (see below), which adjust the weight of the connections on the basis of data. In other words, ANNs 'learn' from examples and have the capability for generalization beyond the training data. In summary a neural network is a massive parallel processor with a natural ability for

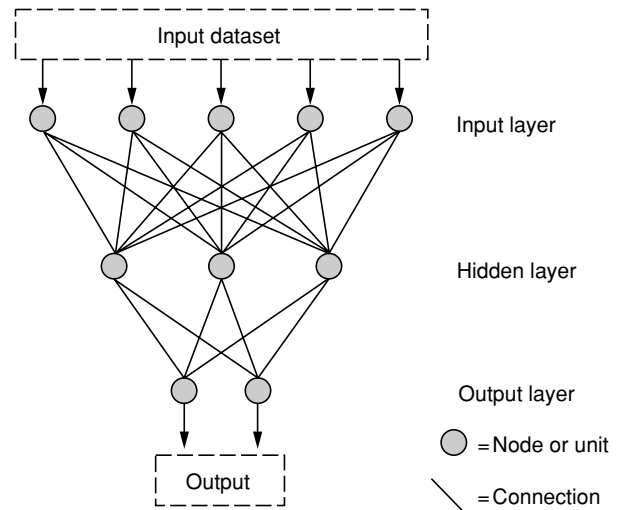


Fig. 1 Example of a neural network with three layers; this structure can be identified as 5-3-2, 5 input nodes, 3 hidden nodes (in only one hidden layer) and 2 output nodes. A network with two hidden layers with three nodes each it would be written as 5-3-3-2.

storing experiential knowledge and making it available for use.

In this study, we have used a feed-forward back propagation neural network (BPN), a powerful system, capable of modelling complex relationship between variables, based on a supervised procedure. The BPN is composed by layers of nodes, where each node is connected to all the nodes of the successive layer, without lateral or feed back connections. The information flow is unidirectional, from the input layer to the output layer, through the hidden layer(s). All the errors that the network makes with the training examples are used to modify the strength of connections between nodes. In particular, each node of the network receives signals coming from the nodes it is connected to. Each input signal is multiplied by the weight assigned to its connection and the weighed signal arrives at the node where it is summed with all the others, this result is then modified by a transfer function (S), called also activation function. The result of the activation function is the node output, which eventually can enter into a new node or the final result (Fig. 2).

There are several transfer functions, but the most common are linear and sigmoid (Fig. 3). In this study, we used the sigmoid transfer function for each node in the hidden and output layers, so the output will be:

$$y = \frac{1}{1 + e^{-a/\rho}}$$

where a is the weighted sum of the inputs to the node.

The ρ coefficient determines the shape of the sigmoid: as ρ increases the curve became flatter. In many cases and

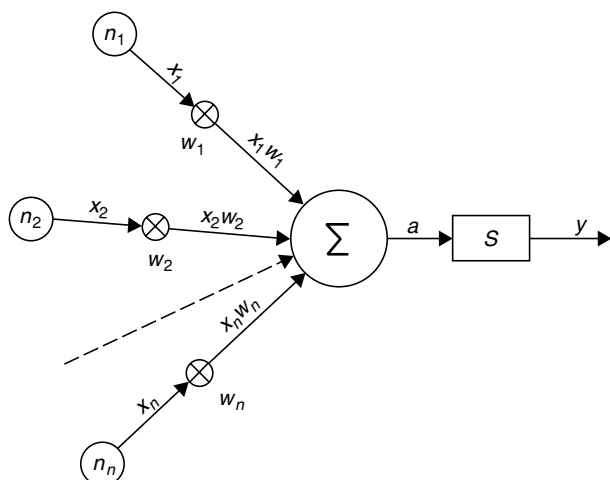


Fig. 2 Block diagram of an artificial neurone. Supposing that there are n inputs with signal $x_1, x_2, x_3, \dots, x_n$ and weights $w_1, w_2, w_3, \dots, w_n$. The weighted sum a , will be $a = x_1w_1 + x_2w_2 + x_3w_3 + \dots + x_nw_n = \sum_{i=1}^n x_iw_i$. The a value, will enter into a transfer function S , and transformed according to different mathematical functions delivering the output y (see text).

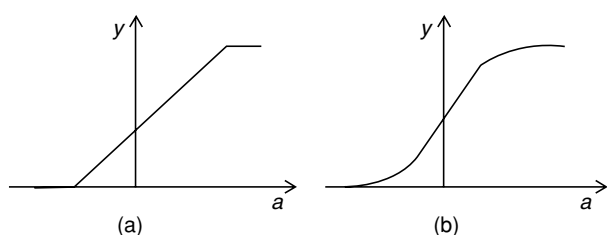


Fig. 3 Examples of (a) linear transfer function, (b) sigmoid transfer function.

also in this study, this parameter is omitted so that it is implicitly assigned the value 1.

Training a neural network A network is trained by providing a set of training examples, one at a time. Each example is composed of all the input and the output values; thus, each input node receives the value of one of the independent variables and the network generates a set of output values by the output nodes. These outputs are the estimates that the network makes of the dependent variables associated with a particular input example.

At the start of network training, the output of the network (actual output) can be very different from the real output (target) of each example. This difference is then used as the basis for a scheme that modifies the network weights with the goal being to minimize this difference. The weights, whose values were randomly assigned at the beginning, were modified according to the error back-propagation rule.

The inputs data were scaled between 0 and 1. This is one of the most common forms of preprocessing of the input variables especially when different variables have typical values, which differ significantly. Two ANNs inputs could be, for example, air temperature expressed in °C and pressure expressed in Pascal; they will have values which differ by several orders of magnitude but their typical size may not reflect a relative importance in determining the required outputs (Bishop, 1995). Also the output values used in the training process were scaled using this procedure and the inverse procedure was used to rescale the output to unit of flux.

The error back-propagation algorithm: For each example p , we have an error E_p , which is a function of the weights. Typically this is defined by the square difference between the actual output y and the target t . Thus, for a single node:

$$E_p = \frac{1}{2}(t - y)^2$$

where y is a function of the weights.

The total error E is then just the sum of the data set errors:

$$E = \sum_p E_p$$

An error is calculated each time the neural network is presented with a training vector and a gradient descent is performed on the error considered as function of the weights. The gradient descent rule technique is based on small changes of opposite sign proportional to first derivative of the function in that point. In this way we get closer and closer to the minimum of the function and once it has been reached, the first derivative in that point equal to zero and the system stop. Thus the function shape slowly modifies (because of the modifications of the other weights), but we will move on it with movements little enough to consider such movements negligible. This could be mathematically expressed as:

$$\Delta w_{kj} = -\eta \frac{dE_{kj}}{dw_{kj}}$$

where η is 'learning rate', a factor that determines the size of the steps that the network takes in navigating through the weight-error function. The size of the learning rate can be set by the user. As a rule, the higher the value of learning rate, the faster the network will locate the point in the weight space that corresponds to the low training error. But there is a penalty for using a value of learning rate too large: the network may continually overshoot the point of minimum error, never reaching it, but bouncing back and forth around it, proceeding chaotically.

In this study, we have overcome the problem related to the size of η by altering the 'pure' gradient descent

training rule to include a portion of last weight change. The new rule is now:

$$\Delta w_{kj}(t) = -\eta \frac{dE_{kj}}{dw_{kj}} + \mu \Delta w_{kj}(t-1)$$

where t is the time and μ is called momentum and its function is to increase the size of the step when the direction, in the weight space, is the same as the direction of the previous step and decreases the size of the step when the directions of the current and previous steps are not the same. The idea is that if the network is making good progress in the current direction then it should keep going forward with an even larger step. If however, conditions have changed between the previous and current step, then take a correspondingly small step.

Datasets and errors At the base of the network training is a dataset made of a series of examples, each one containing the observed inputs and outputs. From these examples, the network is trained with the aim to foresee the output values starting from input values, which have never been seen before, this process is known as generalization. In order to achieve this goal, the network must not learn too much from the examples given during the training, thus losing the capability to generalize on the basis of new examples (overfitting). The training dataset is divided into three groups: *training set*, used for determination of the weights during neural network training, *test set*, used during network training to calculate the errors to prevent overtraining and *validation set*, which was not used at all during training. The purpose of the validation set is to assess the network's performance with 'new' data, which removes the possibility of the network overfitting on training and test sets.

Once the three sets of data have been defined, the training set examples are given to the network and the error between the obtained and the real result is calculated. The modification of the weights occurs after the passage of an *epoch*, that is a number of examples which are set before starting the training and can vary from one to the number of cases in the training set, on the network.

Another parameter, which has to be defined before training, is the number of epochs that have to be processed before the training process stops and the performance of the network evaluated using the test set. The training ends either when an acceptable error level is achieved on the test set or when there is no improvement on the network performances after a certain quantity of epochs has passed. Since this procedure can lead itself to some overfitting to the test set, the performance of the selected network is confirmed by measuring its performance on a third independent set of data called the validation set.

The evaluation of the error made by the network, on both test and validation set, was done through the calculation of different error typologies, we have used:

Pearson correlation coefficient (r)

$$r = \frac{\sum_p (y - \text{mean}(y)) (t - \text{mean}(t))}{\sqrt{\sum_p (y - \text{mean}(y))^2 \sum_p (t - \text{mean}(t))^2}}$$

root mean squared error (RMSE)

$$\text{RMSE} = \sqrt{\frac{\sum_p (y - t)^2}{p}}$$

mean absolute error (MAE)

$$\text{MAE} = \frac{1}{p} \sum_p |y - t|$$

where, p is the number of examples, y is the predicted values and t is the real values.

The dataset used in this study consisted of measurements of CO₂ fluxes taken at 16 European sites using the eddy covariance technique (Aubinet *et al.*, 2000). Since measurements could be, under some circumstances, affected by nighttime stratification and unexpected low eddy flux data, a correction for this flux is needed. The data correction and gap filling had already been done on most sites using multiple regression techniques (Falge *et al.*, 2001) and data were already directly available for elaboration. However, there were four sites where this work had not been done (sites number 2, 4, 6 and 7 of Table 1). For these sites, nighttime values (with $u^* < 0.2$) and other gaps in the data were filled with site-specific neural networks.

The inputs of the network trained for each site were air temperature, air relative humidity, photosynthetically active radiation (PAR) and two series of four fuzzy sets. The fuzzy sets are a way to reduce the linear cumulative numerical weight of time in relation to other variables. In this study, season and time of day were transformed into fuzzy sets. This transformation was made because the progressive numerical increase of time (from day 1 to day 365) is not a meaningful trend, in terms of information, for the network. In each fuzzy set the variable being transformed can take any value between 0 and 1, which represents a degree or percent membership of the original variable value in the fuzzy set.

In this study, the fuzzy transformation was applied in the following way:

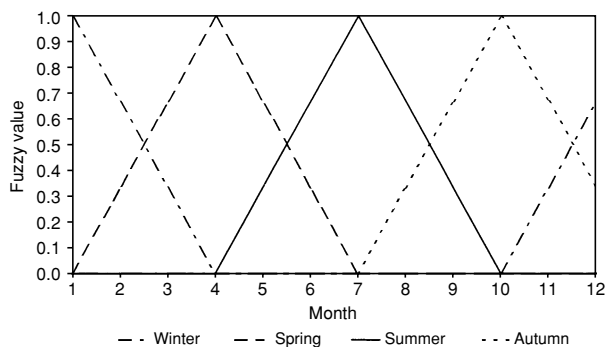
month of the year (Fig. 4)

winter: start in October, maximum in January, end in April

Table 1 Main characteristics of the sites used to estimate the NEE with eddy covariance system

Country	Site name	Latitude	Longitude	Vegetation type	Dominant sp.	Climate*
BE	Brasschaat	51°18'N	04°31'E	Mixed forest	<i>Pinus sylvestris</i> , <i>Quercus robur</i>	T/O
BE	Vielsalm	50°18'N	06°00'E	Mixed forest	<i>Fagus sylvatica</i> , <i>Pseudotsuga menziensis</i>	T
DK	Soroe	55°29'N	11°38'E	Broadleaves deciduous	<i>Fagus sylvatica</i>	T/O
FI	Hyytiälä	61°51'N	24°17'E	Coniferous evergreen	<i>Pinus sylvestris</i>	B
FR	Bordeaux	44°42'N	00°46'W	Coniferous evergreen	<i>Pinus pinaster</i>	T/O
FR	Sarrebouurg	48°40'N	07°05'E	Broadleaves deciduous	<i>Fagus sylvatica</i>	T/S
DE	Tharandt	50°58'N	13°34'E	Coniferous evergreen	<i>Picea abies</i>	T/C
IT	San Rossore	43°43'N	10°17'E	Coniferous evergreen	<i>Pinus pinaster</i>	M
IT	Collelongo	41°50'N	13°35'E	Broadleaves deciduous	<i>Fagus sylvatica</i>	M/Mt
IT	Roccarespampani	42°23'N	11°51'E	Broadleaves deciduous	<i>Quercus cerris</i>	M
IT	Castelporziano	41°45'N	12°22'E	Broadleaves evergreen	<i>Quercus ilex</i>	M
NL	Loobos	52°10'N	05°44'E	Coniferous evergreen	<i>Pinus sylvestris</i>	T/O
SW	Flakaliden	64°14'N	19°46'E	Coniferous evergreen	<i>Picea abies</i>	B/O
SW	Norunda	60°05'N	17°28'E	Coniferous evergreen	<i>Picea abies</i> , <i>Pinus sylvestris</i>	B
UK	Aberfeldy	56°37'N	03°48'E	Coniferous evergreen	<i>Picea sitchensis</i>	T/O
DE	Bayreuth	50°09'N	11°52'E	Coniferous evergreen	<i>Picea abies</i>	T/C

*T, temperate; O, oceanic; B, boreal; C, continental; M, Mediterranean; Mt, montane; S, suboceanic.

**Fig. 4** Fuzzy transformation of the month of the year.

spring: start in January, maximum in April, end in July

summer: start in April, maximum in July, end in October

autumn: start in July, maximum in October, end in January.

So, i.e. May will be 0 winter, 0.667 spring (67%), 0.333 summer (33%) and 0 autumn.

A similar transformation was applied for the time of the day (Fig. 5)

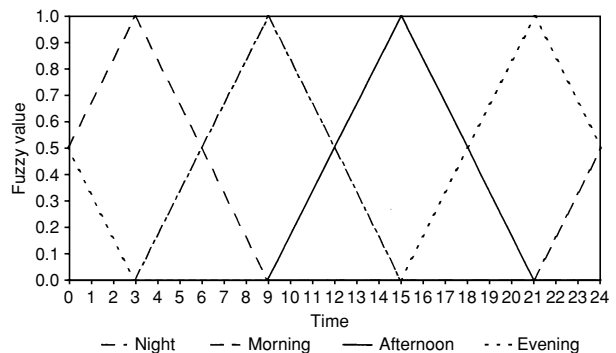
morning: start at 3, maximum at 9, end at 15

afternoon: start at 9, maximum at 15, end at 21

evening: start at 15, maximum at 21, end at 3

night: start at the 21, maximum at the 3, end at the 9.

The original data from each site consisted of about 17500 samples (one measurement every half an hour) but the dataset was composed only by those examples with complete input and output data.

**Fig. 5** Fuzzy transformation of the time of the day.

After the corrections and the gap filling, we estimated the daily NEE for each site. These values were then used for the second part of the work: an assessment of European NEE.

Assessment of European NEE by means of neural networks

In this study, a single network was used to assess NEE of Europe in 1997. The year was split up into 48 periods, four per each month.

The network, with a 12-5-1 structure (Fig. 6), was trained with 760 examples (400 training set, 180 test set, 180 validation set) and generated as output the mean NEE for the period, expressed in gC day^{-1} .

The 12 input nodes used were:

- one for the dew point temperature
- one for the maximum air temperature
- one for the minimum air temperature

- one for the mean air temperature
- one for the maximum Normalized Difference Vegetation Index (NDVI)
- three for the land cover type
- four for the season (fuzzy).

The network structure and the input variables were chosen after trying several networks, with a varying number of hidden nodes and transfer functions. For the input variables, the goal was to find the same meteorological inputs used in the daily application. It was not possible to find PAR or other radiation maps of Europe with weekly time resolution and 1 km of spatial resolution. Other inputs tried were a latitude map and a digital elevation model but they didn't improve the

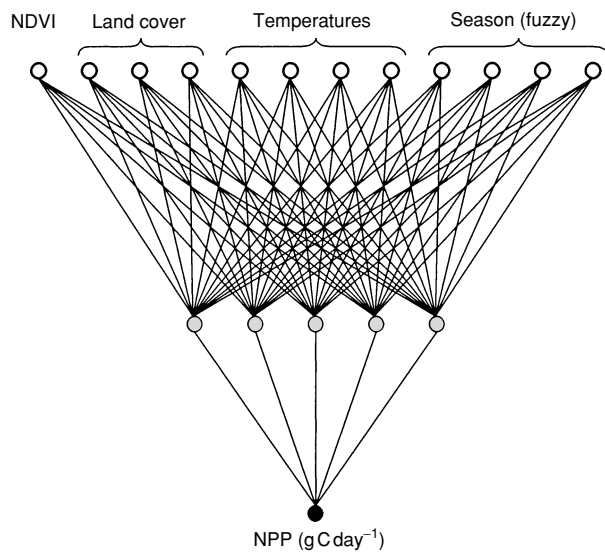


Fig. 6 Scheme of the network used to assess the European NEE.

network's performance. We have used four fuzzy values to predict season. The four fuzzy values used were one of many possible criteria for separating the seasons, for example we could have used other variables such as day length. However, this would be unlikely to improve network performance because the network learns to time season not only from the fuzzy values but also from an integration between all the variables. This is possible because of the many connections between the input, the hidden and the output nodes so that there isn't a variable that guides only one aspect or an aspect guided only from one variable.

Input data A set of input data concerning all the continent, in the form of a set of maps, was needed to train the network and apply it to Europe. The values representing the Euroflux sites positions were extracted from these maps, and these data were used as input for the training process.

In Fig. 7 it is shown the block scheme of preprocessing of the input data to obtain the maps.

Maximum NDVI The NDVI maps used were derived from images acquired by the NOAA-AVHRR sensor (Cracknell, 1997), using bands set to 580–680 nm (R) and 720–1000 nm (NIR), respectively. This satellite acquired one image per day of the same area and had a geometric resolution of about 1.1 km at nadir.

The EDC Distributed Active Archive Center (<http://edcdaac.usgs.gov>) provides compositions obtained by overlaying 10 images of 10 consecutive days from the AVHRR sensor; for each pixel the highest value from the resulting image is taken. Thus, the 10 days composition image is a measure of the maximum value expressed by each pixel in this 10 days period, in each acquisition band. This composition image is also provided for the NDVI, so

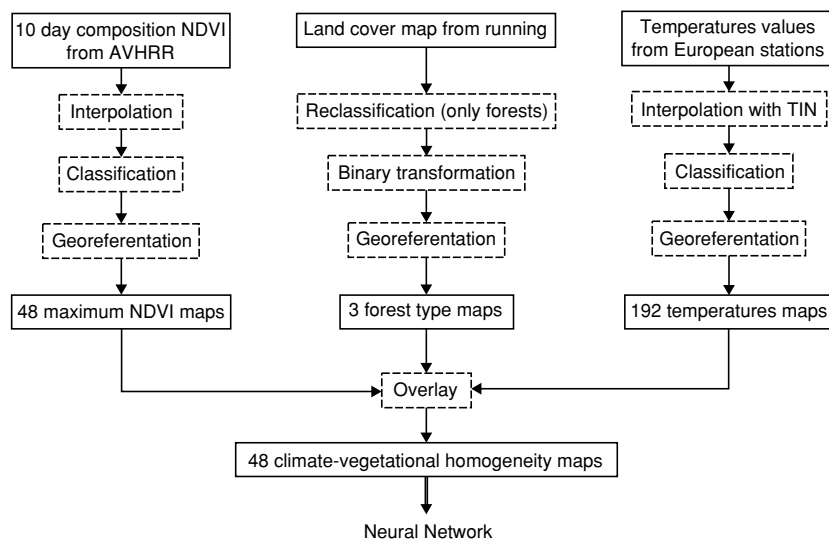


Fig. 7 Block scheme of input data preprocessing.

each pixel is the maximum NDVI value expresses in the 10 days period.

The NDVI maps used in the present work were acquired and elaborated in 1993. For the purpose of the demonstration of the application of the methodology this should not have a major impact on the validity of the present work, however, in the future updated remote sensing products are needed for a better quantification of the sources and sinks distribution. On a 10 days basis the images related to one year are 36 (three each month), but we needed 48 images to complete our dataset, thus the images were interpolated.

Finally, each image was classified in five classes of NDVI distribution.

Temperatures data The climate data used in this work were extracted from the global surface summary of day data produced by the National Climatic Data Center (NCDC, Asheville, USA). This database contained daily summaries of hourly climate data from over 8000 georeferenced worldwide stations, about 3000 of these in Europe. From this database we extracted the dew point, mean, maximum and minimum air temperatures of the European stations together with their geographical coordinates. Then, the mean of each temperature was calculated for each station during all the 48 periods. In total, we obtained 192 values for each station (four temperatures \times 48 periods).

Through Triangulated Irregular Networks (TINs) interpolation method, climatic data were interpolated across Europe.

With this procedure, we created 192 maps of European temperatures, four for each of the 48 periods. Also these temperatures maps were further reclassified in 12 classes.

Land cover The most accurate map for Europe is the Corine Land Cover but unfortunately this map does not cover all Europe and for this reason Corine was discarded. For the purpose of this study, the Vegetation Lifeforms map (Running *et al.*, 1994) was used.

The Vegetation Lifeforms map has seven cover types:

1. Evergreen Needleleaf Vegetation
2. Evergreen Broadleaf Vegetation
3. Deciduous Needleleaf Vegetation
4. Deciduous Broadleaf Vegetation
5. Annual Broadleaf Vegetation
6. Annual Grass Vegetation
7. Non-vegetated Land
8. Water Bodies

Our work focused only on forests thus we reclassified it into only three classes: evergreen broadleaf, deciduous broadleaf and evergreen needleleaf. The deciduous needleleaf class was added to the deciduous broadleaf because there are no eddy flux stations in this forest

type. This problem was minor because the presence of deciduous needleleaf forest is not extensive in Europe.

The land cover map thus modified, was converted in a set of three binary images, with value 0 for false and 1 for true, each of these concerning the presence or absence of one of the three-forest cover type.

Georeferencing In order to work with all the eight layers at the same time, the eight maps created needed to be georeferenced. As the original maps used different projections it was impossible to overlay them. Consequently, a set of about 70 ground control points spread in Europe, a third order mapping function and the latitude longitude reference system were used for georeferencing. The error in the output maps was less than 1%, due principally to the different geometric resolution of the input images.

Layers overlay For all the 48 periods, the eight layers were overlaid to create a new map where the classes were the result of each combination among the input map classes resulting in a climate-vegetation homogeneity classification (CVHC). Each class of each of the new maps (48 new maps, one for each period) was characterized by 12 values: eight from the maps (four for the temperatures, three for the forest type and one for the NDVI) and four from the fuzzy values of the season of the period.

Finally the network was trained and applied using this input data to reproduce an estimate of NEE for each class of the CVHC.

Results and discussion

Gap filling at each flux tower site

Before spatializing NEE data across Europe, gap filling of night time fluxes at some sites was necessary. Nighttime fluxes and gaps in data acquisition were filled with a specific neural network application. Figure 8 shows an example of the application of neural network generated data for site four (Bordeaux) where the model data are compared with the real eddy flux dataset not used during the training phase. Thus this represents the real performance of the generalization. Figure 9 shows an example of generalization of a comparison of daily trends in real and ANN data.

Despite some days with calm night where ANN and real data behave differently, due to the fact that real data are not u^* corrected, the agreement between data and ANN is remarkable. It is worth to notice that ANN predictions tend to discard noisy data that are unlikely to represent real processes.

The synthesis of the gap filling procedure and error analysis for four sites is presented in Table 2. For all the sites the Pearson coefficient was above 0.81 indicating a good agreement between the ANN and real data.

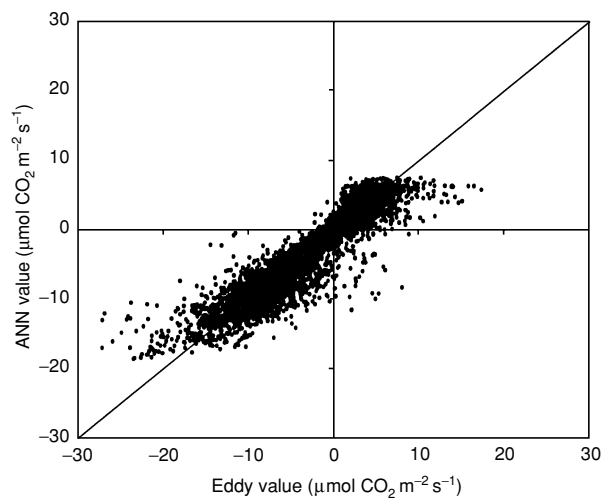


Fig. 8 Eddy vs. ANN flux values for validation dataset. Site number 4 (Bordeaux). Also shown is a 1 : 1 line.

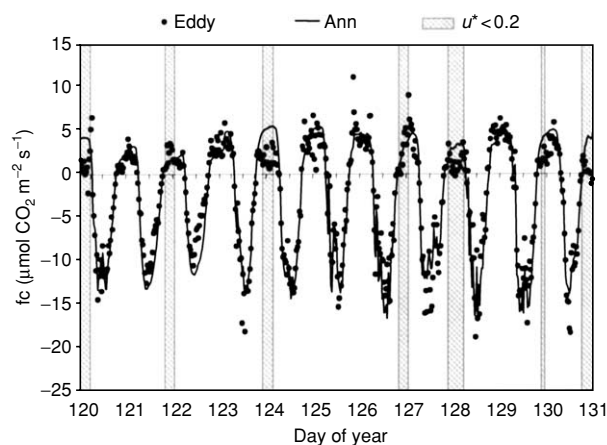


Fig. 9 Eddy vs. ANN daily trend for a 10 days period.

Table 2 Gap filling summary for four sites

	Castelporziano	Bordeaux	Flakaliden	Norunda
Examples with $u^* > 0.2$	9045	11372	13573	13441
Validation dataset	3729	5221	5459	5374
	<i>Data type</i>	<i>Data type</i>	<i>Data type</i>	<i>Data type</i>
Mean	-3.611	-2.241	-0.641	0.181
STD	5.925	6.550	3.532	8.659
Minimum value	-21.35	-33.45	-28.68	-49.85
Maximum value	14.53	44.58	24.76	65.38
	<i>Errors</i>	<i>Errors</i>	<i>Errors</i>	<i>Errors</i>
Pearson	0.887	0.916	0.845	0.813
RMSE	2.766	2.489	1.897	5.000
MAE	2.029	1.662	1.135	3.358

Data and errors analysis. Values in $\mu\text{mol CO}_2 \text{m}^{-2} \text{s}^{-1}$.

The examples above highlight the efficiency of ANN for data recovery and gap filling. Ultimately, ANNs may prove to be superior to the normal regression or modelling approaches for data recovery and gap filling. (Van Wijk & Bouten, 1999; Falge *et al.*, 2001).

NEE spatialization with ANN

In order to scale up the single flux tower data to the European continent, a single ANN was created using all the 16 flux sites datasets. In this case the training and validation was created with weekly data. Figure 10

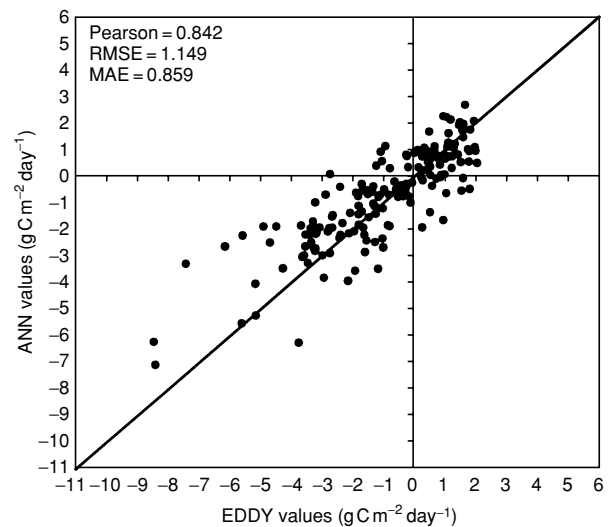


Fig. 10 Eddy vs. ANN NEE values for validation dataset. Also shown is a 1 : 1 line.

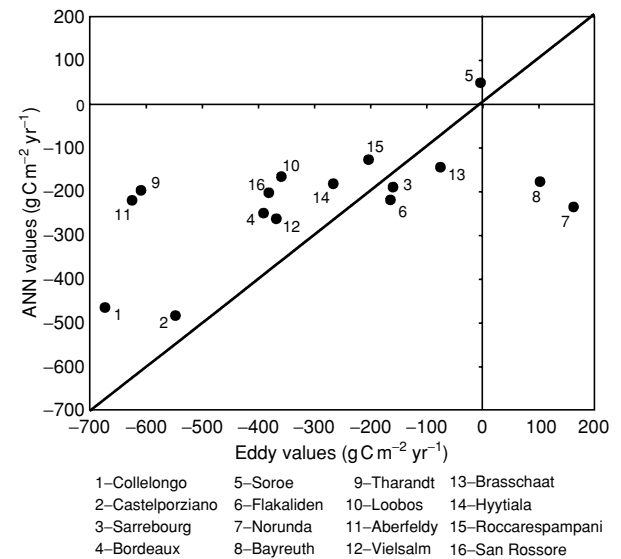


Fig. 11 Eddy vs. ANN NEE annual sum values for the 16 training sites. Also shown is a 1 : 1 line.

shows the comparison between the ANN generalization and the real data, not used during the training phase.

A comparison between annual sums of NEE, derived from the same ANN, and real data is shown in Fig. 11. For this data there was a clear decrease in the predictive power of ANN. However, an in depth look to the site specific data highlights how several sites may be outliers, in particular 7 (Norunda), 8 (Bayreuth), 9 (Tharandt) and 11 (Aberfeldy).

Site 7 is unique in the network since it is the only site that is proved by ecological considerations to be a source of carbon (Lindroth *et al.*, 1998) (while site 8 also appears to be a carbon source there are particular problems at this site, see below). Site 7 also exhibits high interannual variability. Site 11 is an artificial plantation of fast growing

species, which has previously been shown to be an outlier in the latitudinal trend of this dataset (Valentini *et al.*, 2000). Site 8 has been reanalysed recently and shown to have a heterogeneous canopy with a problematic fetch (T. Foken, personal communication). The reasons for site 9 being an outlier are not clear, however, an eddy covariance software intercomparison for this site showed the greater departure from the mean (EUROFLUX, 1999).

The differences between ANN estimates of annual NEE and real data can also be partially attributed to the fact that we have used a single network for all the sites. Consequently, some of the data from the sites identified as outliers could not be reproduced well. This finding highlights how ANNs will be useful for detecting noise (outliers) from an underlying signal. However, difference

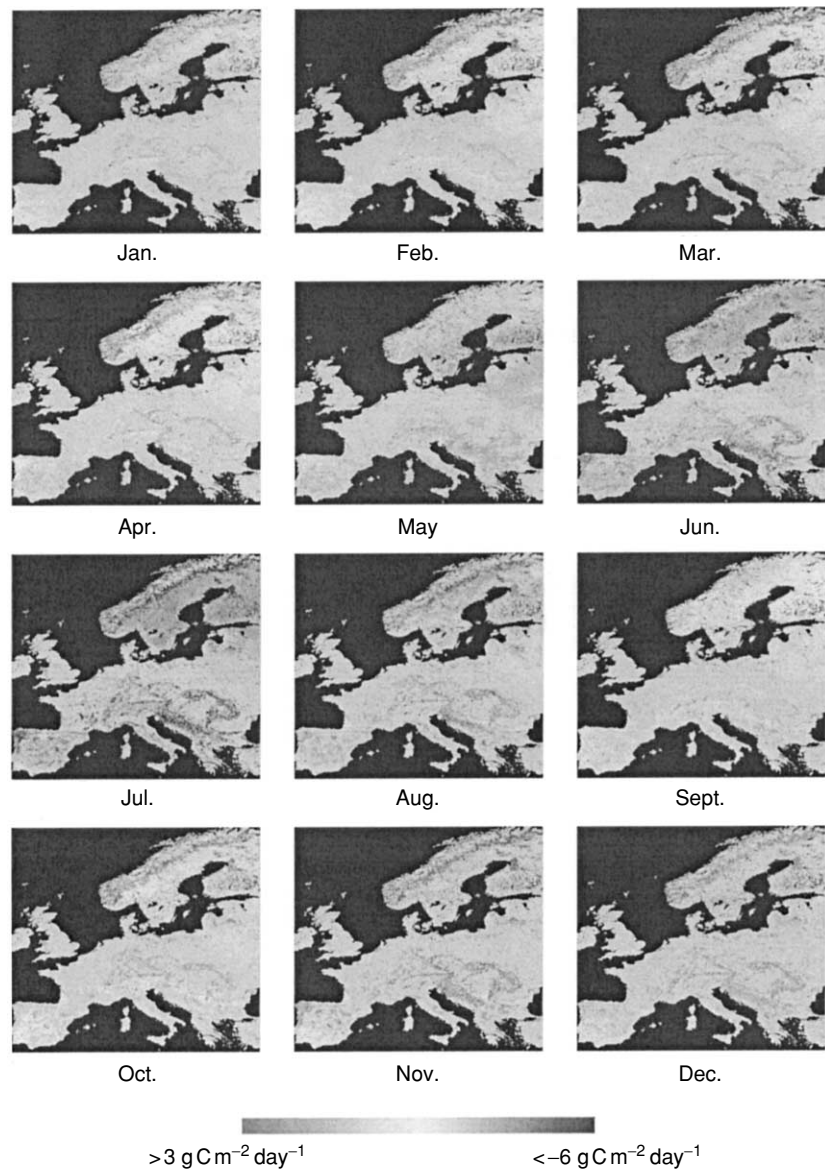


Fig. 12 Examples of NEE maps generated. Each figure shows second week of each month.

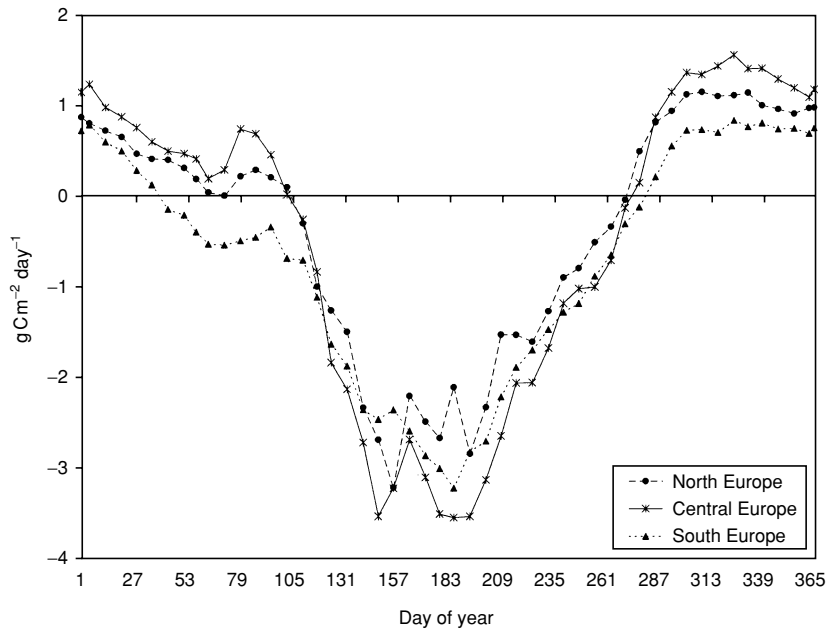


Fig. 13 Daily average carbon balance per ground unit, divided in north ($>52^{\circ}\text{N}$), central ($52^{\circ}\text{--}44^{\circ}\text{N}$), and south Europe ($<44^{\circ}\text{N}$).

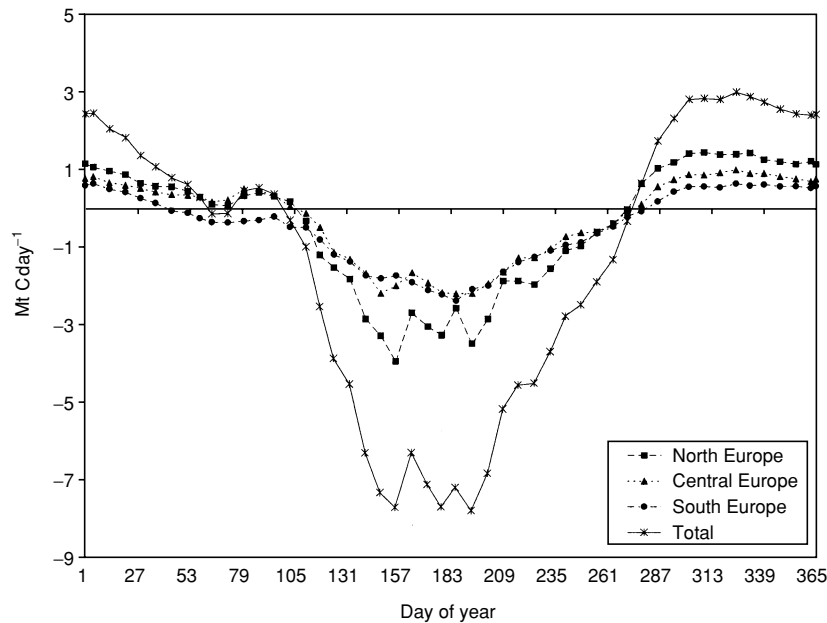


Fig. 14 Daily average carbon balance for cumulative forest area in north, central, and south Europe.

between short- and long-time (as annual) performance was found also by Barciela *et al.* (1999) modelling ocean productivity.

Figure 12 shows the final monthly estimates of NEE for Europe derived from ANN. The overall European carbon uptake from this analysis was $0.47 \text{ Gt C yr}^{-1}$. This value is within the range of $0.2\text{--}0.7 \text{ Gt C yr}^{-1}$ for Europe reported recently for several techniques (Schulze *et al.*, 2001).

An analysis of the forest carbon exchange per unit of ground (m^2) is presented in Fig. 13, according to three latitude classes ($>52^{\circ}$, $52^{\circ}\text{--}44^{\circ}$, $<44^{\circ}$). At all latitudes

there is a pulse of respiration in spring. This sudden increase of respiration may be due to increased construction respiration at the onset of the season. This effect has been clearly shown at leaf scale for deciduous species, where an increase in respiration was measured before bud burst and also during leaf expansion (Schulze & Koch, 1971). It is however, interesting to see it at the continental scale as a coherent functional response. Thus this is an example where a 'biological' signal at leaf scale can have a significant effect in driving continental biosphere – atmosphere fluxes.

The other interesting feature is that the length of the growing season is longer in the south of Europe of about 32 weeks, compared with north and central Europe which have a similar length growing season of about 27 weeks.

When expressed per unit ground area the northern forests of Europe exhibit the lowest rate of carbon uptake (Fig. 13). However, due to the large spatial extent they represent the largest component of the European carbon sink (Fig. 14).

Conclusions

In this study, we have presented ANNs as a new method for estimating forest ecosystem fluxes at European scale. ANN may have significant advantages over traditional modelling techniques and represent a change in the philosophy of model development for biospheric fluxes towards a strong emphasis on feedbacks with observational data as a 'constraint' for predictions. This study has shown that ANNs may be particularly useful at the single site level for optimizing the gap filling procedures. They may offer the best performance and be used as a routine system for gap filling. Weekly data spatialization (one general ANN for all the sites) predictions were good but could be further improved with additional and better quality input data. In particular (1) in this study, the land cover representation was coarse, (2) NDVI could be obtained in real time, (3) more sites are becoming available for ANN training and (4) solar radiation inputs could be added. The ANN outputs for annual sums of NEP were not of the same quality as the high temporal frequency data. However, the discrepancies were largely due to the incorporation of sites with known problems of data interpretation. This study shows that ANN methods have a clear capacity to extract outliers and specific behaviours, which can be used for the improvement of process description. Another potential use of ANN could be to combine observations and modelling outputs to improve atmospheric and biospheric models parameterization.

Acknowledgements

We thank all EUROFLUX project PIs for having provided a unique dataset and continue to work hard within the CARBOEUROFLUX project. This work has been funded by EC projects CARBOEUROFLUX (EVK2-CT-1999-00032) and CARBODATA (EVK2-CT-1999-00044) of the European Community. We also wish to thank FLUXNET for having largely created the conditions to build up the community of flux people and the

integrated data analysis. We thank Martin Heimann, Philippe Ciais and Ray Leuning for stimulating discussions on this topic. We also wish to thank Dr Graham Hymus who revised the manuscript making it more clear and readable.

References

- Aubinet M, Grelle A, Ibrom A *et al.* (2000) Estimates of the annual net carbon and water exchange of forests: the EUROFLUX methodology. *Advances in Ecological Research*, **30**, 113–175.
- Barciela RM, Garcia E, Feràndez E (1999) Modelling primary production in a coastal embayment affected by upwelling using dynamic ecosystem models and artificial neural networks. *Ecological Modelling*, **120**, 199–211.
- Bishop CM (1995) *Neural Networks for Pattern Recognition*. 482pp, Oxford University Press, New York.
- Bousquet P, Peylin P, Ciais P *et al.* (2000) Regional changes in carbon dioxide fluxes of land and oceans since 1980. *Science*, **290**, 1342–1346.
- Cracknell AP (1997) *The Advanced Very High Resolution Radiometer*. Taylor & Francis.
- Cramer W, Bondeau A, Woodward FI *et al.* (2001) Global response of terrestrial ecosystem structure and function to CO₂ and climate change: results from six dynamic global vegetation models. *Global Change Biology*, **7**, 357–373.
- Demuth H, Beale M (2000) *Neural Network Toolbox – For use with MATLAB, Version 4*. The Math Works Inc., Natick.
- EUROFLUX (1999) *ENV4-CT95-0078, Final Report*. European Commission, Directorate General for Research, Belgium.
- Falge E, Baldocchi D, Olso R *et al.* (2001) Gap filling strategies for defensible annual sums of net ecosystem exchange. *Agricultural and Forest Meteorology*, **107**, 43–69.
- Lek S, Guégan JF (2000) *Artificial Neuronal Networks – Application to Ecology and Evolution*. 262pp, Springer, Berlin.
- Lindroth A, Grelle A, Morén AS (1998) Long-term measurements of boreal forest carbon balance reveal large temperature sensitivity. *Global Change Biology*, **4**, 443–450.
- Running SW, Loveland TR, Pierce LL (1994) A vegetation classification logic based on remote sensing for use in global biogeochemical models. *Ambio*, **23** (1), 77–81.
- Schulze ED, Dolman AJ, Jarvis P *et al.* (2001) *The Carbon Sink: Absorption Capacity of the European Terrestrial Biosphere*. EUR19883, European Commission, Directorate-General for Research, Luxembourg.
- Schulze E-D, Koch W (1971) Measurement of primary production with curettes. In: *Productivity of Forest Ecosystems. Proceedings of the Brussels Symposium 1969*. UNESCO, pp. 141–157.
- Valentini R, Matteucci G, Dolman AJ *et al.* (2000) Respiration as the main determinant of carbon balance in European forests. *Nature*, **404**, 861–865.
- Van Wijk MT, Bouten W (1999) Water and carbon fluxes above European coniferous forests modelled with artificial neural networks. *Ecological Modelling*, **120**, 181–197.